621.914.5:621.833

Paper No. 180-26

GRAPHIC ANALYSIS OF HOBBING IN UNFINISHED SPACE*

By Kenichi TERASHIMA**, Taku UENO***

and Kazunori HIDAKA****

A new graphic method is proposed, in which the hobbing state in the unfinished tooth space can be easily illustrated through simple calculations and with only one tooth profile template.

This method is useful not only in the estimations of the cutting thickness, length and zone in various hobbings but also in the forecast of the chip flowing on the rake face. The tooth wear can be also related analytically with the cutting amount and the chip flowing. Additionally, several tooth profiles developed for the anti-wear purpose are discussed.

1. Introduction

In order to reduce the hob wear and to increase the machining efficiency, many hobbing tests have been made, but by trial and error method. Even if good results are obtained from experiments, the reasons have often been explained only by conjecture, because it is very difficult to analyze numerically the hobbing mechanism in the unfinished space and it is impossible to observe the cutting behavior in the invisible hob gash crossed with the gear space.

The hobbing behavior in the unfinished space is influenced by many hobbing factors, such as module, number of teeth and helix angle of gear; outside diameter, number of threads and rake angle of hob; feed and its direction, etc[1]. The hob wear also varies on each tooth and the chip flow on the rake face which affects the tooth wear varies with gear materials, cutting oil and other factors[2]. Therefore, even if the effective methods are obtained on one hobbing condition, these are not always effective on the other hobbings.

In the previous paper[3], a numerical analysis method was proposed for the quantitative solution of this problem. But, in this method, a larger capacity computer must be applied even for the analysis of standard tooth profile hob, and especially for the effect analysis of different profiles, the larger capacity is required.

This paper demonstrates a new graphic method which can be easily drawn with the programmable microcomputer and with only one template; and by this method the cutting thickness, length and the chip flow of the hob developed for the anti-wear purpose can be visually understood.

The symbols and the hobbing conditions used in this paper are shown in Table 1, and the definitions of + or - sign are shown in Table 2.

Table 1 Symbols and hobbing test

	Symbols	Hobbing test
Common	m : Module	* 4 mm
	α_o: Pressure angle	* 20°
	Γ : Setting angle	
	a : Center distance	
	Δa: Addendum shift	* 0
Gear	Z : Number of teeth	* 33
	β : Helix angle	* (Spur) 0°
	R_k: Outside radius	Gear materials S45C-H
	R_o: Pitch circle radius	Hardness Hв 250
	R_r: Root circle radius	
	R_g: Base circle radius	
Hob	r_k: Outside radius	* 50 mm
	r_o: Pitch circle radius	
	r_e: r_o - (dedendum)	
	Z_w: Number of threads	* 1 RH
	G_n: Number of gashes	* 11
	γ : Lead angle	
	γ_e: Lead angle on r_e circle	
	δ : Rake angle	* 0°
	$\bar{\beta}$: Helix angle of gash	* 0°
	sl: Whole depth	Hob materials SKH55 HrC 64
	Δt: Tooth distance on axis	
	$\Delta\theta$: Tooth division angle	
	N : Tooth profile	Standard
Cutting	$+f$: Conventional cut feed	* -2 mm
	$-f$: Climb cut feed	
	Θ : Revolution angle of gear	v = 51 m/min
	θ : Revolution angle of hob	

Table 2 Definitions of ± in symbils

Symbols	±
Δa	According to ± of addendum shift
β $\bar{\beta}$	Right hand : +
γ γe	Right hand : +
δ ω	According to ± of rake angle
Γ	According to ± of ($\beta - \gamma$)
Θ	Righthand rev. of x axis : +
θ	Down ward from horizontal plane : +
N	Right side from 0-th tooth : +
f	Conventional cut : +

* Received 15th August, 1978.

** Professor, Faculty of Engineering, Nagasaki University.

*** Professor, Faculty of Engineering, Kyushu University.

**** Associate Professor, Sasebo Technical college, Sasebo-City.

2. Graphic analysis method

The hobbing is a complicated three-dimensional motion which is related to many items shown in Table 1. Accordingly, the hobbing cannot be treated without a sort of simplification so as to illustrate it on one plane. Fortunately the limit of the drawing accuracy is up to the four figures, so that the approximation to such a degree is allowable.

Figure 1 shows a state in which a gear having right helix angle β, module m and number of teeth Z is conventionally hobbed under feed f and addendum shift Δa with a hob of outside radius r_k, number of right helical threads Z_w, number of gashes G_n and rake angle δ.

Under such conditions, the graphic method will be described. Tooth number N, tooth interval Δp, position ΔtN and $\Delta\theta N$, and others also are illustrated in Fig.1.

2.1 The basic theory of graphic analysis

The conception of this graphic analysis is explained in Fig.4 and Fig.6, where $\bar{N}$th tooth is one whose cutting behavior has to be referred to. The top and the bottom centers V, W[Fig.4(a)] of $\bar{N}$th tooth are respectively in a state where the tooth $\bar{N}$ cut down by θi more after cutting deepest into the gear. An imaginary cone with the same axis as the gear one contains V and W on its surface and revolves with the gear. Such cones are set by putting $\theta i = \theta_0$, θ_1, θ_2, $\cdots$ in order. With the hob revolution, both centers of $\bar{N}$th tooth pass through the cone surface at the same time. The hob is inclined by the setting angle Γ, so that when the top center of each tooth reaches the cone surface, a locus of bottom center moves as shown in Fig.4(b). To be illustrated on a plane, every bottom center is rotated about the corresponding top center up to the cone surface.

The cone surface P is revolved about the top center V'' cut deepest into the P surface up to horizontal plane P', and then this is projected on a plane P''. The P'' plane is the drawing one and the center loci on each cone are obtained on one plane (Fig.6).

After the top and the bottom centers of the tooth profile template (Fig.5) are superposed respectively at the corresponding centers on the drawing plane, the whole template profile is traced. The traced profile can be considered the cutting zone when the tooth passes through the cone surface. Geometric shapes of the gear and the hob can be calculated by * symbols given in Table 1, and the following constants are found.

$$\gamma = \sin^{-1}(0.5mZ_w/r_0),\ \gamma_e = \tan^{-1}(r_0\tan\gamma/r_e)$$
$$\Delta p = 2\pi r_0\cos\gamma\{1+\tan\gamma\tan(\gamma+\bar{\beta})\}/G_n$$
$$\Delta t = \Delta p\sin\gamma,\ \Delta\theta = \Delta p\cos\gamma/\gamma_0,\ \Gamma = \beta - \gamma$$
$$\omega = \sin^{-1}(r_k\sin\delta/r_e) - \delta,\ a = R_0 + r_0 + \Delta a$$
$$K_1 = Z_w/Z/\{1-f\sin\beta/(\pi mZ)\},\ K_2 = 0.5K_1 f/\pi \quad \cdots\cdots\cdots(1)$$

Here K_1 is the revolution ratio of gear and hob, K_2 is the feed ratio per unit revolution (rad.) of hob. The helical gashes with helix angle $\bar{\beta}$ are treated as the segments of straight gash arranged in turn along helix gash. In Figure 2, the gear coordinates $x_g y_g z_g$ are fixed in the hobbing system, the tooth space coordinates $x_s y_s z_s$ exist at the height of $Z_g = h$ and rotate with the gear, and the tooth profile center line of 0th tooth and the tooth space center line y_s meet with common normal line y_g at the height $Z_g = 0$. If the hob is reversed by $(\Delta\theta N - \theta)$ from the above state, Nth tooth comes into a state in which the tooth cuts down by θ. Then, the center axis y_s of tooth space on a plane of height h exists at the angular distance Θ from y_g-axis.

$$\Theta = K_1(\Delta\theta N - \theta) + h\tan\beta/R_0 \quad \cdots\cdots\cdots(2)$$

In this case, the gear coordinates of top center $x_{gt} y_{gt} z_{gt}$ and bottom center $x_{gr} y_{gr} z_{gr}$ are obtained from the ellipse motions of both centers (Fig.3).

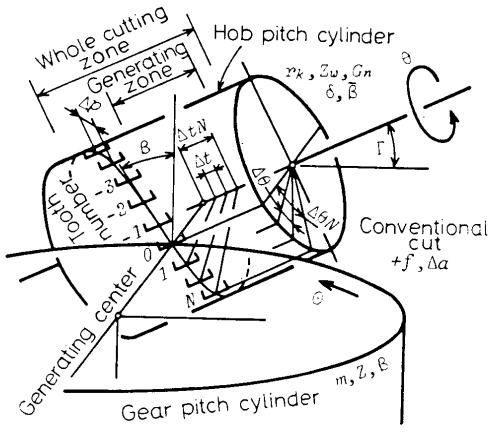

Fig.1 Tooth number N, position of Nth tooth (ΔtN, $\Delta\theta N$)

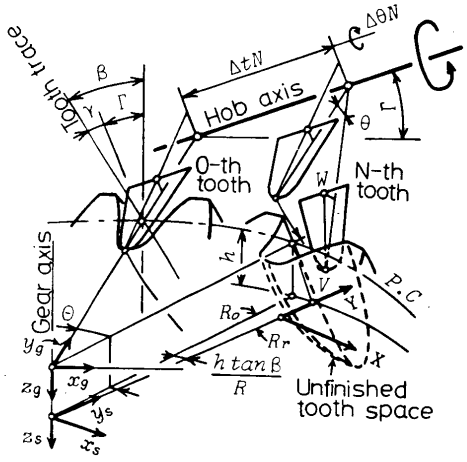

Fig.2 Coordinate systems

$$x_{gt} = \Delta tN\cos\Gamma + r_k\sin\theta\sin\Gamma$$
$$y_{gt} = a - r_k\cos\theta$$
$$z_{gt} = -\Delta tN\sin\Gamma + r_k\sin\theta\cos\Gamma - K_2(\Delta\theta N - \theta)$$
$$x_{gr} = \Delta tN\cos\Gamma + r_e\sin(\theta-\omega)\sin\Gamma$$
$$y_{gr} = a - r_e\cos(\theta-\omega)$$
$$z_{gr} = -\Delta tN\sin\Gamma + r_e\sin(\theta-\omega)\cos\Gamma - K_2(\Delta\theta N - \theta) \quad \cdots\cdots\cdots(3)$$

Putting $N = \bar{N}$ and $\theta = \theta_i$, the coefficients $\bar{a}$ and $\bar{b}$ at an intersection $z_g = \bar{a}y_g + \bar{b}$ [Fig.4 (a)] of cone surface and plane $y_g z_g$ can be calculated as follows.

$$\bar{R}_t = \sqrt{x_{gt}^2 + y_{gt}^2}, \quad R_r = \sqrt{x_{gr}^2 + y_{gr}^2}$$
$$\bar{a} = (z_{gr} - z_{gt})/(\bar{R}_r - \bar{R}_t), \quad \bar{b} = z_{gt} - \bar{a}y_{gt}$$
$$h_i = \bar{a}R_0 + \bar{b}, \quad \zeta = \tan^{-1}|\bar{a}| \quad \cdots\cdots\cdots(4)$$

When the top center of $\bar{N}$th tooth contacts the cone surface set as θ_i, the revolution angle θ is found from Eq.(5), $x_{gt}y_{gt}z_{gt}$ from Eq.(3) and z_c from R in Eq.(5). Until an accurate value of θ is obtained, the calculation satisfying $|z_{gt} - z_c| <$ allowable value ε in Eq.(5) must be repeated with the θ value varied.

$$R = \sqrt{x_{gt}^2 + y_{gt}^2}, \quad z_c = \bar{a}R + \bar{b}$$

$|z_{gt} - z_c| \leqq \varepsilon$: Top of tooth exists on the cone face.

$|z_{gt} - z_c| > \varepsilon$: Eq.(3) and (5) is repeated in next θ

$$\theta = \sin^{-1}\{(\Delta tN\sin\Gamma + z_c)/(r_k\cos\Gamma)\} \quad \cdots\cdots\cdots(5)$$

The coordinates of both centers are found from Eq.(3) under the obtained θ, and then these are shown on the tooth space coordinates. Here, the tooth space exists at a directional angle Θ described by Eq.(2) where h_i in Eq.(4) and θ in Eq.(5) are respectively used as h and θ.

$$x_s = x_g\cos\Theta - y_g\sin\Theta, \quad y_s = x_g\sin\Theta + y_g\cos\Theta \quad \cdots\cdots\cdots(6)$$

Next, the top center is projected on a contact plane P of a cone generating line which passes through an intersection of the space center line y_s on the plane h_i and the cone surface set as θ_i. The bottom center is rotated up to P-plane [Fig.4(c)] and then is revolved again about the top center whose tooth cuts closest to the cone vertex up to horizontal plane P' parallel to $x_s y_s$ plane [Fig.4(b)].

In the coordinates XY (Fig.2) on the drawing plane P'', Y axis is the space center line y_s and X is the tangent to the dedendum circle. Finally, the above centers are projected on the plane P'' and are represented by XY.

$$\Delta Y = (y_{st} - \bar{y}_{st})(1/\cos\zeta - 1)$$
$$X_t = X_{st}, \quad Y_t = y_{st} + \Delta Y - R_r, \quad X_r = x_{sr}$$
$$Y_r = \sqrt{s_l - (x_{st} - x_{sr})^2} + y_{st} + \Delta Y - R_r$$

$\bar{y}_{st}$: y_s coordinate of deepest tooth $\cdots\cdots\cdots(7)$

Thus, the loci of all centers can be plotted on the drawing plane. A flow chart of this calculation is shown in Table 3.

2.2 The drawing procedure

(1) Magnification of figure

All the drawings are magnified to module 80 mm, because these can be drawn on A3 section paper, which is convenient in size. Additionally, the drawings and their analyses become easy and the figure accuracy increases by magnifying. Moreover, drawings in various modules are possible using only one 80 module template.

(2) Tooth profile template (Fig.5)

A tracing paper on which the tooth profile of module 80 is accurately drawn

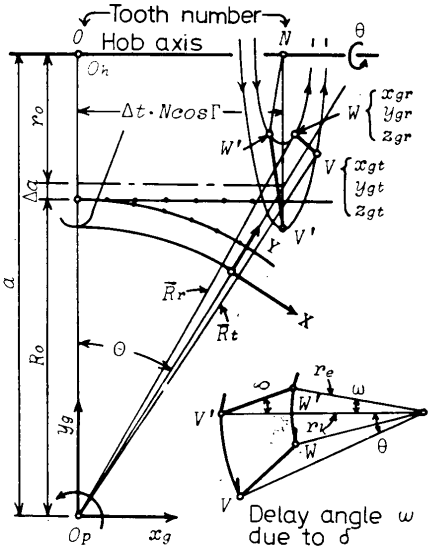

Fig.3 Revolutions of the top and the bottom centers

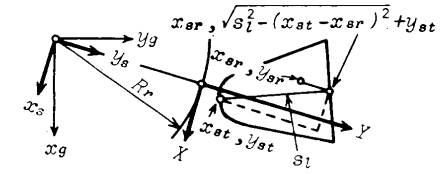

(c) Revolution view and its projection

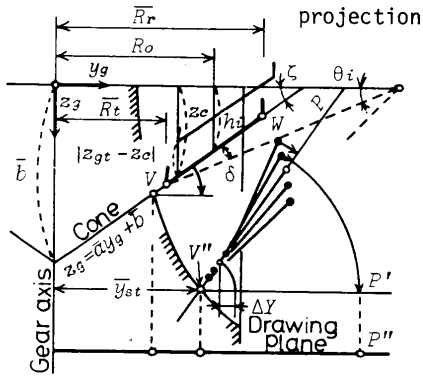

(a) Imaginary cone

(b) Fan-shape of the bottom centers, and their revolution

Some parts of figure are expressed approximately to the explanation

Fig.4 Imaginary cone and drawing plane

is stuck in an A4 sized celluloid holder, and then two templates are made from both sides at the same time by using the cutter and the file. The scales divided along the tooth profile are convenient for understanding the cutting position. The bottom points 1 and 6 of the raked hob are shifted by $r_e\omega\tan\gamma_e$ in the right or the left direction. In case of a modified profile, the same ones are made only as the template.

(3) Selections of the tooth $\bar{N}$ and angles θ_i setting the cone

In order to analyze the cutting states of all the teeth, the 0th tooth may be selected as $\bar{N}$, and if the cutting state of a certain fixed tooth is closely examined, its tooth number must be chosen. The setting angle θ_i of an imaginary cone can be better increased in 5° steps, until R_t in Eq.(4) becomes larger than R_k. The setting end is generally expected to be within about 35°.

(4) Tooth space profile before one revolution of gear (Fig.6)

It is necessary that the profiles of the unfinished tooth space before one revolution be found on each cone surface. In the conventional hobbing, the hob before one gear revolution is higher by feed f than hob position after one revolution, so that all the center coordinates before one revolution must be calculated by putting respectively $h+f$ as h in Eq.(1) and z_c+f as z_c in Eq.(5).

These are plotted on the section paper (symbol ∘ in Fig.6). After both centers of the template are superposed on the corresponding points, the whole template profile is traced. An envelope of the traced profiles becomes the space profile on each cone before one revolution.

(5) Cutting section of Nth tooth (Fig.7)

The center coordinates are calculated in case that the hob is set at the generating center, and are plotted on the same section paper as the space profile was drawn.

Table 3 Calculation of center co-ordinates

Read hobbing conditions Common : m, α_c Gear : Z, β Hob : r_k, δ, Z_w, G_n, $\bar{\beta}$, $\bar{N}$ Cutting : $\pm f$, Δa
Calculation of basic constants Gear : R_o, R_k, R_r, R_g, a Hob : r_o, r_e, γ, sl, γ_e Δp, Δt, $\Delta\theta$, N_o, N_r, Γ, ω
N_o, N_r [3]
Setting of imaginary cone $\bar{a}\,\bar{b}\,\bar{h}$ with respected to $\bar{N}$ and θ_i
Calculation of center co-ordinates Center co-ordinates of each tooth are calculated every θ_i in cutting before one revolution and cutting of this time through Eqs.(3)~(6)
Drawing with XY plotter

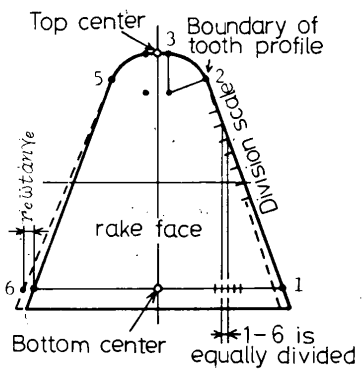

Fig.5 Tooth profile template

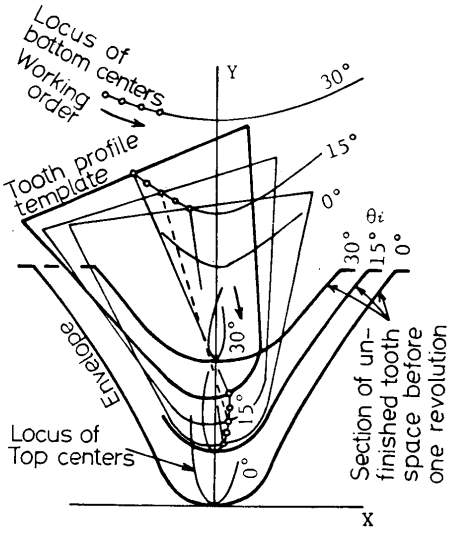

Fig.6 Center loci before one revolution of gear and sections of the tooth space on θ_i cone

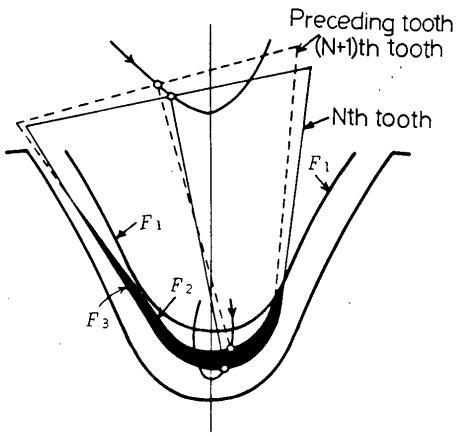

Fig.7 Section to be removed with Nth tooth

When the template profiles are traced from the most preceding tooth to Nth tooth, then a cutting zone of Nth tooth is a blacked portion enclosing three profiles F_1, F_2, F_3. F_1 is the space section generated before one revolution, F_2 is an envelope generated from the most preceding tooth to $(N+1)$th tooth and F_3 is the Nth tooth profile.

(6) Multi-pass hobbing

In the twice pass hobbing, for example, if the first passing is made under the half cutting depth whose addendum shift Δa is equal to 2.25/2 module, a tooth space removed by the space profile shifted by Δa is hobbed in the second passing.

2.3 Accuracy of graphic analysis

Figure 8 shows an example (0th tooth was selected as $\bar{N}$) illustrating the 4th tooth whose corner wear is very large in the hobbing of Table 1. Figure 9 shows a result calculated strictly under the same condition through the numerical analysis[3].

In Fig.8, the hobbing state in the unfinished space is seen from the upper side in gear axis direction. Figure 9 is seen in radius direction. The cutting progresses from 33° to 0° because of climb hobbing. The top edge only works slightly from 33° to 25° and the side edges begin to cut at 25°.

The cutting state in Fig.8 corresponds nearly to that in Fig.9. Marks ▽ and ▼ denote respectively the right and the left corner. The cutting width along the tooth profile becomes widest at 15°. At this angle, the cutting thickness of the left side edge is closely two times as thick as that of the right edge.

The top and both side edges work separately from 15°. These two figures agree well in the cutting zone, thickness and others. In the practical hobbing under the condition shown in Table 1, the rubbing mark of chips and the cutting zone on the rake face also agree with the states in both figures.

According to the principle applied in this analysis, the smaller the number of teeth Z is, and the larger the angle β is and the farther the distance from tooth $\bar{N}$ is, the larger the drawing errors are. Because these errors occur mainly in the direction of tooth thickness, the error influences are relatively small and their effects are confirmed even in comparison of the hobbing tests and the drawn figures.

Accordingly, the calculation can be made as simple as possible; that is, the feed less than 2 ~ 3 mm may be neglected, the helical gears less than $\beta = 15°$ may be replaced by their equivalent spur gear under the feed $f/\cos\beta$, the helix gashes less than $\bar{\beta} = 5°$ can be regarded as straight ones and the rake angles less than $\delta = 10°$ may be neglected. Such approximations are useful enough to analyze the hobbing behavior in the unfinished space.

3. Applications of graphic analysis

3.1 A cause analysis of the corner wear

Figure 10 shows the wear state of the

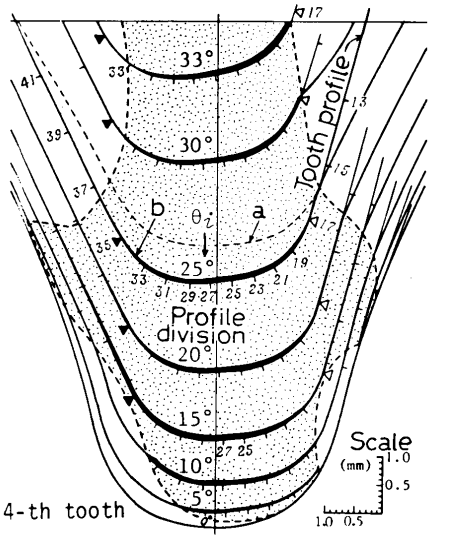

Fig.8 Cutting state with 4th tooth (standard tooth profile)

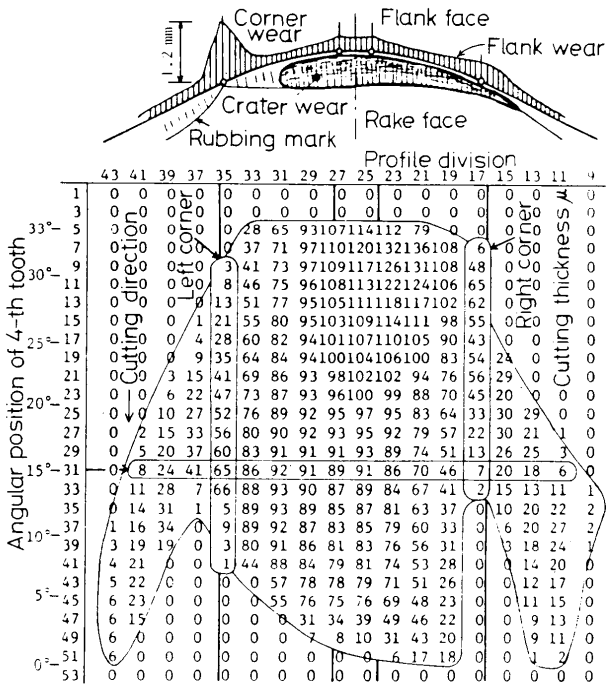

Fig.9 The numerically analyzed cutting state with 4th tooth

4th tooth, where a crater wear extends as far as the right corner in spite of the thin cutting thickness, and a gently sloping wear occurs on its flank. The white mark rubbed by the chip flow becomes narrow suddenly near the left corner. The cutting thickness is thicker at this corner and an unusually large wear occurs triangularly on this flank.

The growth mechanism of the corner wear has not been clarified enough. The rubbing phenomena between the left corner ▼ and the unfinished space surface before one revolution can not be considered from the graphically analyzed result (Fig.8). The cutting amounts of corners ▼▽ are respectively about one-third as much as that of the top, whereas the wear of corner flank is several times wider than that of the top. Moreover, an unusual triangular wear arises only at the left corner in spite of the same cutting amount.

Figure 11 illustrates, in relation to Fig.8, a process in which a chip is generated from the space surface with the 4th tooth. Since only the top edge works slightly from 33° to 25°, the chip flows out from the top edge [Fig.(a)]. At 25°, the chip begins to flow out from both side edges too, and the cutting width reaches a maximum at 15°. The chip from the right edge is thin, so its interference is also small, and the right chip is pushed aside by the top chip flow.

But the chip from the left is thick, so that its interference is also larger. Thus, the chip flows both from the top and from the left have to stand up folded at the corner from the rake face. The chip at the folded lower end is hardened by the difficult flowing out and the large cutting force. This is a cause of the corner wear, which was reported in another paper .

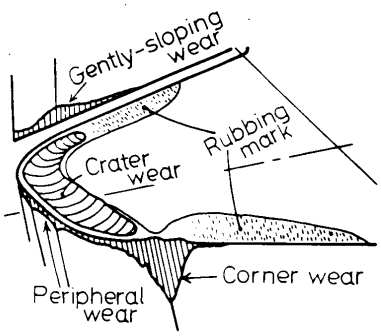

Fig.10 Wear of 4th tooth

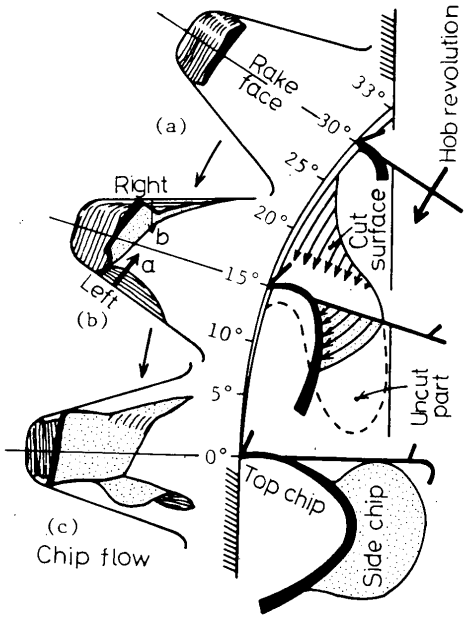

a : Large interference
b : Small interference

Fig.11 Process generating the chip

3.2 Tooth profiles modified for the anti-corner-wear purpose

Figures 12～14 show some examples of the tooth profile developed to reduce the corner wears by controlling the interferences of the chips flowing out from the top and from the side edges. Now these hobs are said to reduce not only the wear but the cutting force and the vibration. Three tooth profiles modified from the standard

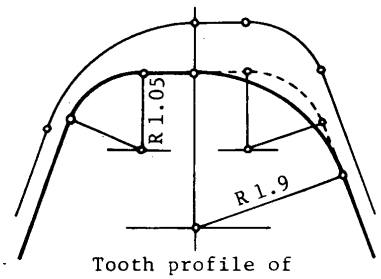

Tooth profile of different nose hob

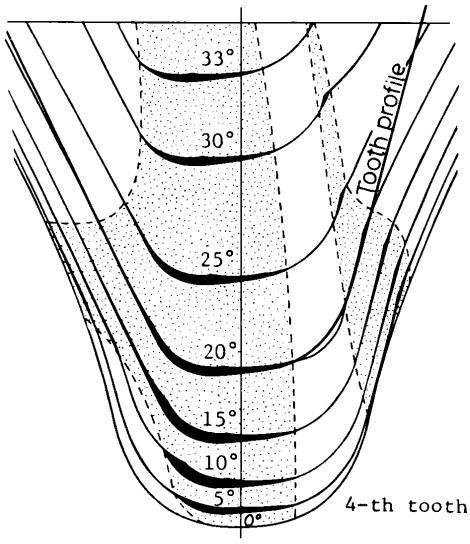

Fig.12 Different nose hob

one in Fig.8, are developed for anti-wear purpose and are investigated through the graphic analyses and the hobbing experiments under the condition in Table 1.

(1) Different nose hob (Fig.12)

A tooth profile of this hob has different radii for the right and the left tip round, and both sides of this profile are alternately arranged along the hob thread. Both round edges work alternately in the right and in the left, so that a chip is separated into two parts on the larger radius corner. Thus the chip interference from the right side edge is prevented.

The smaller radius edge cuts excessively the portion uncut with the large radius edge of the preceding tooth. The chip thickness on this corner is thicker, so that its flowing power becomes strong and the chip flows diagonally pushed to both sides. As a result, the chip interference from large round is removed and the corner wear is also reduced on the small round flank.

(2) Three chip hob[1] (Fig.13)

This hob is developed through the analyses of the corner wear. Both tip rounds of its profile have two concaves with different phases. It will be easily understood from the tooth profile that the chip is separated into three pieces by both concaves, and the chip interferences from the top and both sides are perfectly prevented. The cutting oil also will permeate easily into the cutting portion, so that the corner wear and the cutting force will be reduced too. About 0.05 mm roughness was expected to remain on the gear tooth fillets, but this roughness of the produced gears was difficult to distinguish visibly.

(3) Surfy hob[1] (Fig.14)

This hob has a tooth profile with small waves touching internally the standard tooth profile, and is used only in rough hobbing. It is understood from the tooth profile that many chips like slender pieces are cut off by the wave tops. Mutual interference of the chips is perfectly prevented, and the cutting oil also infiltrates easily. Accordingly, needless to mention, the tooth wear, the cutting force and the cutting vibration become little.

3.3 Analyses of the cutting force and the torque

Figure 15 shows the sectional areas to be cut (the parts blacked in Figs.8 and 14) and the area moment of the cut section with respect to the hob sxis. After each section is magnified 10 times (module 800) and is separated into several simple areas, the sectional areas are measured. Area moment is obtained by multipiying the sectional area by radius from hob axis.

The sectional area multiplied by the

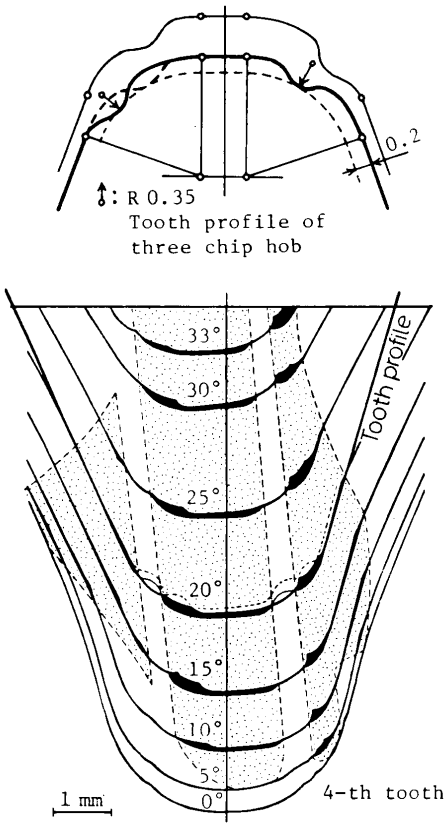

Fig.13 Three chip hob

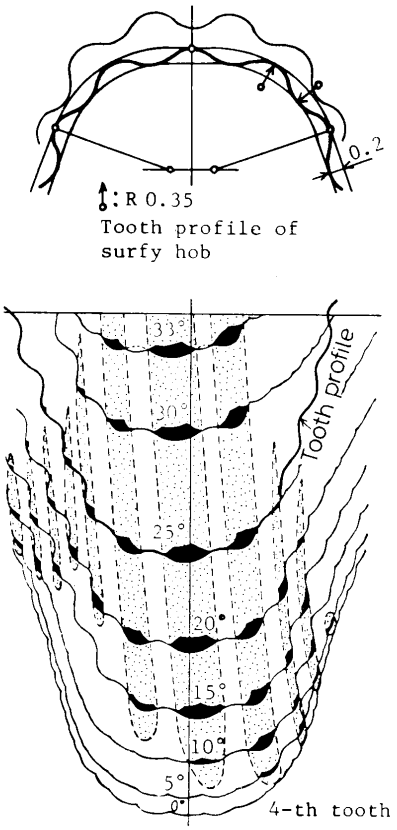

Fig.14 Surfy hob

specific cutting resistance makes the cutting resistance and the cutting resistance multiplied by a radius from hob axis to area center becomes the cutting torque. But the cutting thickness and the section area vary every moment by the hob revolution, and the value of specific cutting resistance changes widely depending on whether the chip flow is disturbed by interference or not.

The specific cutting resistance calculated from the actually measured torque of the atandard tooth (Fig.8 and Fig.15) was in the range of 228 ~ 347 kgf/mm^2.

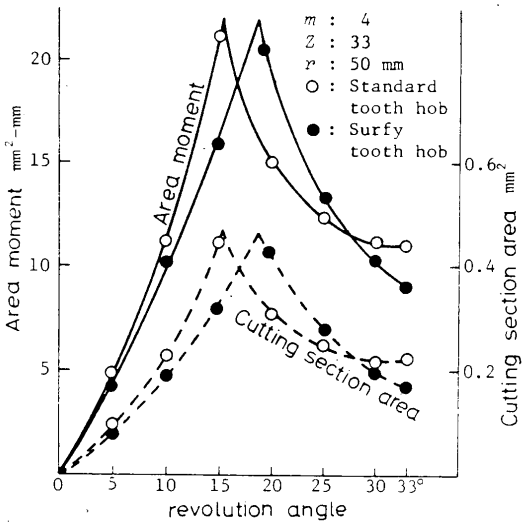

Fig.15 Cutting section area and its area moment

4. Conclutions

The hobbing state in the unfinished tooth space has been able to be expressed graphically through the simple calculation and with only one template. The conclutions of this paper are summarized as follows.

(1) This graphic method can be applied to various hobbings such as hobbing of the spur gear or the helical one with the multi-threaded, the helix gashed, the raked and the tapered hob under the conventional, the climb, or the multi-pass cut.

(2) Cutting zone of each tooth, cutting thickness, its width along the tooth profile, its peripheral length, and so on can be visibly observed through this analysis.

(3) The wear causes can be made clear by connecting the practical wear to the cutting state figure, and the chip flow causing a corner wear can be foreseen on the rake face.

(4) This method will be able to analyze as well the wear cause, the cutting torque, the cutting vibration and others.

Acknowledgement

Authors would like to thank KOBE SEIKO Co. and AZUMI Co. for preparing the various hobs.

References

(1) Hidaka, K., et al., Trans. Japan Soc. Mech. Engrs. (in Japanese), Vol.44, No.388(1978 - 12), p.4359.
(2) Hidaka, K., et al., Trans. Japan Soc. Mech. Engrs. (in Japanese), Vol.45, No.389(1979 - 1), p.129.
(3) Terashima, K. and Ueno, T., Bulletin of the JSME (in English), Vol.21, No. 155 (1978 - 5), p.907.